Article

Kinetics of the Interconversion of Parahydrogen and Orthohydrogen Catalyzed by Paramagnetic Complex Ions

Mitsuru Matsumoto, and James H. Espenson

J. Am. Chem. Soc., **2005**, 127 (32), 11447-11453• DOI: 10.1021/ja0524292 • Publication Date (Web): 26 July 2005

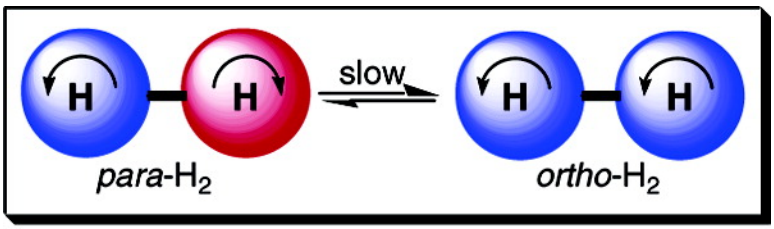

$$\text{H-H} + \text{Cat} \underset{k_b}{\overset{k_f}{\rightleftharpoons}} \text{H-H} + \text{Cat}$$

$$k^0 (= k_f + k_b) \propto \frac{\mu^2}{r^6}$$

More About This Article

Additional resources and features associated with this article are available within the HTML version:

- Supporting Information
- Links to the 4 articles that cite this article, as of the time of this article download
- Access to high resolution figures
- Links to articles and content related to this article
- Copyright permission to reproduce figures and/or text from this article

View the Full Text HTML

J|A|C|S
ARTICLES
Published on Web 07/26/2005

Kinetics of the Interconversion of Parahydrogen and Orthohydrogen Catalyzed by Paramagnetic Complex Ions

Mitsuru Matsumoto and James H. Espenson*

Contribution from the Department of Chemistry, Iowa State University of Science and Technology, Ames, Iowa 50011

Received April 14, 2005; E-mail: espenson@iastate.edu

Abstract: The rate constants of para-/orthohydrogen (*p*-/*o*-H_2) nuclear spin isomerization have been measured by means of ^{1}H NMR in deuterated solvents at 298.2 K. The indicated reaction is catalyzed by paramagnetic complex ions giving rate constants that are proportional to the concentrations of the catalysts. The second-order rate constants are directly proportional to the squares of the magnetic moments for the solvated metal complexes for two classifications: $M(solv)_m^{2+}$, M = 3*d* transition metals; $Ln(solv)_n^{3+}$, where in 1:9 D_2O-CD_3CN the aqua complexes are the predominant species, Ln = lanthanides. The other 3*d* transition metal complexes with different ligands show rate constants that also depend on the sizes of ligands. Whereas the correlation between the second-order rate constants and magnetic moments is consistent with Wigner's theory, the size of catalyst shows a more modest effect on the rate constants than expected. The effective collision radii of the complexes, calculated from the rate constants, proved to be approximately constant for each series of solvated metal complexes.

Introduction

Molecular hydrogen comprises two nuclear spin isomers, parahydrogen with opposed nuclear spins and orthohydrogen with parallel nuclear spins. At $T > 298$ K the equilibrium proportions are precisely 1 para:3 ortho, and this mixture is referred to as "Normal Hydrogen."[1] Below that temperature the equilibrium ratio follows the van't Hoff equation, such that an approximate 1:1 equilibrium ratio exists at liquid nitrogen temperature.

$$\textit{para}\text{-}H_2 \leftrightarrows \textit{ortho}\text{-}H_2$$

$$K_{po} = k_{po}/k_{op} = 3.00 \text{ at } 298 \text{ K} \qquad (1)$$

Although nuclear spin interconversion occurs slowly in the gas phase owing to the involvement of a forbidden triplet−singlet transition, the reaction can be catalyzed by various solids and paramagnetic species. At present, many experimental[2−7] and theoretical[8−11] studies have been done with solid-state catalysts or at solid catalyst surfaces. In solution, the spin conversion via H_2 coordination to a diamagnetic catalyst has drawn the major amount of attention,[12−14] due to the utilizable parahydrogen induced polarization phenomenon (PHIP).[15,16] On the other hand, research on paramagnetic catalysis in solution has been limited to the early investigations of Farkas[17−20] and Wilmarth.[21−23] Despite the limited techniques then available, these authors observed a qualitative correlation between the rate constants and the magnetic moments of the catalysts.

In this article we present a comprehensive report of para-/orthohydrogen (*p*-/*o*-H_2) nuclear spin isomerization, catalyzed by various paramagnetic species studied by the use of ^{1}H NMR spectroscopy. Wigner's theory was used to analyze the rate constants in terms of variations in magnetic moments and radii.[24]

Experimental Section

Cylinder hydrogen (99.5%) was purified through a "De-oxo" device (Matheson, Oxygen remover Model 64-1008A) and an activated Molecular Sieves/Drierite column and then further dried through a liquid nitrogen trap packed with glass wool. The purified normal hydrogen (25% *p*-H_2) was converted to *para*-enriched hydrogen (50% *p*-H_2) by

(1) Greenwood, N. N. E. A. *Chemistry of the Elements*, 2nd ed.; Butterworth-Heinemann: Oxford, 1997.
(2) Andrews, L.; Wang, X. *Rev. Sci. Instrum.* **2004**, *75*, 3039−3044.
(3) Strzhemechny, M. A.; Hemley, R. J. *Phys. Rev. Lett.* **2000**, *85*, 5595−5598.
(4) Shevtsov, V.; Malmi, P.; Ylinen, E.; Punkkinen, M. *Physica B* **2000**, *284*−*288*, 385−386.
(5) Grazzi, F.; Ulivi, L. *Europhys. Lett.* **2000**, *52*, 564−570.
(6) Juarez, A. M.; Cubric, D.; King, G. C. *Meas. Sci. Technol.* **2002**, *13*, N52−N55.
(7) Tezuka, Y.; Kanesaka, I.; Toyooka, K.; Takeuch, Y. *Z. Physik. Chem.* **1972**, 210−219.
(8) Shevtsov, V.; Ylinen, E.; Malmi, P.; Punkkinen, M. *Phys. Rev. B* **2000**, *62*, 12386−12394.
(9) Buchachenko, A. L.; Berdinsky, V. L. *J. Phys. Chem. B* **1996**, *100*, 18292−18299.
(10) Ilisca, E.; Bahloul, K.; Rami, M. *J. Phys. B* **1996**, *29*, 607−625.
(11) Ilisca, E. *Prog. Surface Sci.* **1992**, *41*, 217−335.
(12) Matthes, J.; Pery, T.; Gründemann, S.; Buntkowsky, G.; Sabo-Etienne, S.; Chaudret, B.; Limbach, H.-H. *J. Am. Chem. Soc.* **2004**, *126*, 8366−8367.
(13) Brown, J. M.; Canning, L. R.; Downs, A. J.; Forster, A. M. *J. Organomet. Chem.* **1983**, *255*, 103−111.
(14) Tadros, M. E.; Vaska, L. *J. Colloid Interface Sci.* **1982**, *85*, 389−410.
(15) Eisenberg, R. *Acc. Chem. Res.* **1991**, *24*, 110−116.
(16) Blazina, D.; Duckett, S. B.; Dunne, J. P.; C., G. *J. Chem. Soc., Dalton Trans.* **2004**, 2601−2609.
(17) Farkas, L.; Sachsse, H. *Z. Phys. Chem.* **1933**, *B23*, 19−27.
(18) Farkas, L.; Garbatski, U. *J. Chem. Phys.* **1938**, *6*, 260−263.
(19) Farkas, L.; Garbatski, U. *J. Chem. Phys.* **1938**, *6*, 904.
(20) Farkas, L.; Garbatski, U. *Trans. Faraday Soc.* **1939**, *35*, 263−268.
(21) Claeys, Y.; Baes, C. F., Jr.; Wilmarth, W. K. *J. Chem. Phys.* **1948**, *16*, 425−426.
(22) Wilmarth, W. K.; Baes, C. F., Jr. *J. Chem. Phys.* **1952**, *20*, 116−121.
(23) Wilmarth, W. K.; Barsh, M. K. *J. Am. Chem. Soc.* **1953**, *75*, 2237−2242.
(24) Wigner, E. *Z. Phys. Chem.* **1933**, *B23*, 28−32.

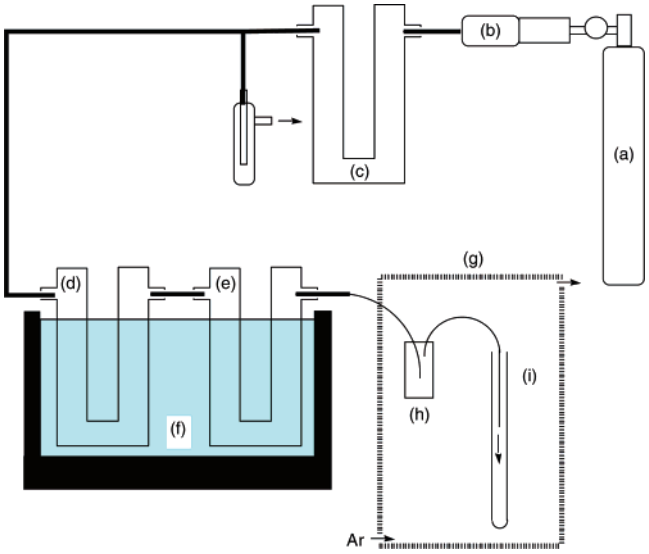

Figure 1. Setup for the preparation of *para*-enriched hydrogen solution. (a) hydrogen gas cylinder, (b) "De-oxo" device, (c) Molecular Sieves/ Drierite column, (d) glass wool column, (e) Fe_2O_3 column, (f) Liq. N_2 pool, (g) glovebag, (h) dust trap, (i) 5 mm NMR tube with a J. Young valve.

passing it over chunks of iron(III) oxide (Aldrich 99.8%) at liquid nitrogen temperature, as shown schematically in Figure 1.

Entire sample preparations were carried out under an argon atmosphere. A sample solution was first degassed with Ar scrubbing, and then *para*-enriched hydrogen gas was bubbled into the sample through the septum seal. The growth of the ^{1}H NMR resonance of *o*-H_2 (*p*-H_2 is ^{1}H NMR inactive) at δ 4.47−4.62 was then recorded as a function of time.

In this study, O_2 must be excluded for two reasons: (i) as a paramagnetic species, O_2 can catalyze the *p*-/*o*-H_2 spin conversion in the gas phase;[17,25] (ii) O_2 oxidizes some of the divalent 3*d* transition metal complexes, which results in false rate constants. To avoid aerial O_2 contamination, all the glass and glass-copper tubing joints were sealed with Torr-Seal (Varian), and an inert atmosphere in the glovebag was maintained by an Ar stream. A 5 mm NMR tube equipped with a J. Young valve (Wilmad) was used for kinetic measurements.

Acetonitrile-d_3 (CIL, 99.8 atom % D), deuterium oxide (Aldrich, >99.96 atom % D), dimethylformamide-d_7 (Aldrich, 99.5 atom % D), trifluoromethanesulfonic acid (HOTf, Aldrich, 98%, $OTf^- = CF_3SO_3^-$), tetrabutylammonium hexafluorophosphate (Bu_4NPF_6, Aldrich, 98%), $Cu(OTf)_2$ (Aldrich, 98%), $FeCp_2$ (ferrocene, Aldrich, 98%), $CoCl_2 \cdot 6H_2O$ (Fisher, 98.1%), and iron(III) perchlorate hydrate (Aldrich), were used without further purification.

Metal triflates ($M(OTf)_2$; M = Mn, Fe, Co, Ni, Zn) were prepared by adding an excess amount of HOTf to the appropriate metal chloride or carbonate.[26,27] Argon gas was passed through the solution for >1 h while it was heated to >60 °C. The solution was dried at 150 °C under reduced pressure. The salt obtained was dissolved in the minimum amount of 1 mM HOTf, and the filtrate dried at 150 °C under reduced pressure for 5 h. Lanthanide(III) triflates, $Ln(OTf)_3$, were prepared in the same manner but starting with high-purity (>99.99%) lanthanide oxides (Ln_2O_3) obtained from the Ames Laboratory's Material Preparation Center.

$Ni(OTf)_2$ was recrystallized from 1 mM HOTf/D_2O solution and dried under Ar stream to obtain $Ni(OTf)_2 \cdot 6D_2O$. $V(BF_4)_2 \cdot 6H_2O$,[28] $VO(OTf)_2 \cdot 10H_2O$,[29] $Cr(OTf)_2 \cdot 13H_2O$,[30] $[Co(phen)_3](ClO_4)_2 \cdot 3H_2O$,[31] $[Cr(NCCD_3)_6](OTf)_3$,[32] $[Cr(bpy)_3](ClO_4)_3$,[33] and $[Cu(cyclam)](OTf)_2$[34] were synthesized according to the literature methods.

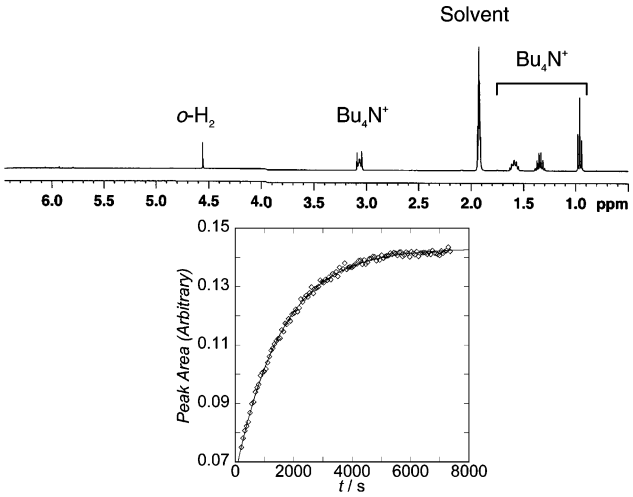

Figure 2. ^{1}H NMR spectrum of *o*-H_2 in acetonitrile-d_3 and the kinetic trace from the peak area of *o*-H_2. T = 298.2 K. The sample contains 4.58 × 10^{-3} mol L^{-1} of $Co(NCCD_3)_6^{2+}$ as the catalyst and 3.04 × 10^{-3} mol L^{-1} of Bu_4NPF_6 as a reference.

Measurements with 3*d* transition metal catalysts were carried out in acetonitrile-d_3 where the solubility of hydrogen is ca. 8 times higher than that in water, thus increasing the signal-to-noise ratio and the precision of the data. For lanthanide complexes as the catalysts, the use of a mixed solvent D_2O:acetonitrile-d_3 =10:90 (v/v) was required owing to the poor solubility of anhydrous $Ln(OTf)_3$ in acetonitrile-d_3. Despite the use of a mixed solvent, the preference for O-donors over monodentate N-donors is so pronounced for the lanthanides that the predominant species is taken to be $[Ln(OD_2)_n]^{3+}$, where *n* likely progresses 10−9−8 along the series.[35,36] Solutions were acidified by HOTf if necessary.

Results and Discussion

Spin Conversion Reactions with Divalent 3*d* Transition Metal Complexes. A sharp ^{1}H NMR signal of orthohydrogen was observed around δ = 4.6 throughout this study. The peak area of *o*-H_2 appeared to be rather sensitive to the nature of solutes and their concentrations; therefore a quantitative analysis of molecular hydrogen concentration was not attempted.

The time course ^{1}H NMR spectrum of *o*-H_2 is shown in Figure 2, in which the sample solution contains $Co(OTf)_2$ ($OTf^- = CF_3SO_3^-$) as the catalyst and tetrabutylammonium hexafluorophosphate (Bu_4NPF_6) as the NMR reference. The rate of equilibration follows first-order kinetics, yielding values of observed rate constants k_{obs} that varied linearly with the concentrations of $Co(NCCD_3)_6^{2+}$.

The rate constants calculated from each kinetic trace are proportional to the concentration of the catalyst, but no effect was found from the addition of acid (HOTf), diamagnetic species ($Zn(OTf)_2$ and $FeCp_2$), or Bu_4NPF_6; see Figure 3. The lack of the $Zn(OTf)_2$ and HOTf concentration dependences on

(25) Farkas, A.; Farkas, L. *Proc. R. Soc. London, Ser. A* **1935**, *154*, 152−157.
(26) Dixon, N. E.; Lawrence, G. A.; Lay, P. A.; Sargeson, A. M.; Taube, H. *Inorg. Synth.* **1986**, *24*, 243−250.
(27) Heintz, R. A.; Smith, J. A.; Szalay, P. S.; Weisgerber, A.; Dunbar, K. R.; Beck, K.; Coucouvanis, D. *Inorg. Synth.* **2002**, *33*, 75−83.
(28) Holt, D. G. L.; Larkworthy, L. F.; Povey, D. C.; Smith, G. W. *Inorg. Chim. Acta* **1990**, *169*, 201−205.
(29) Richens, D. T.; Harmer, M. A.; Sykes, A. G. *J. Chem. Soc., Dalton Trans.* **1984**, 2099−2105.
(30) Cantuel, M.; Bernardinelli, G.; Imbert, D.; Bünzli, J.-C. G.; Hopfgartner, G.; Piguet, C. *J. Chem. Soc., Dalton Trans.* **2002**, 1929−1940.
(31) Burstall, F. H.; Nyholm, R. S. *J. Chem, Soc.* **1952**, 3570−3579.
(32) Lo, S. T. D.; Swaddle, T. W. *Inorg. Chem.* **1975**, *14*, 1878−1881.
(33) Baker, B. R.; Mehta, B. D. *Inorg. Chem.* **1965**, *4*, 848−854.
(34) Scott, M. J.; Holm, R. H. *J. Am. Chem. Soc.* **1994**, *116*, 11357−11367.
(35) Richens, D. T. *The Chemistry of Aqua Ions*; Wiley: Chichester, U.K., 1997.
(36) Dunand, F. A.; Helm, L.; E., M. A. *Adv. Inorg. Chem.* **2003**, *54*, 1−69.

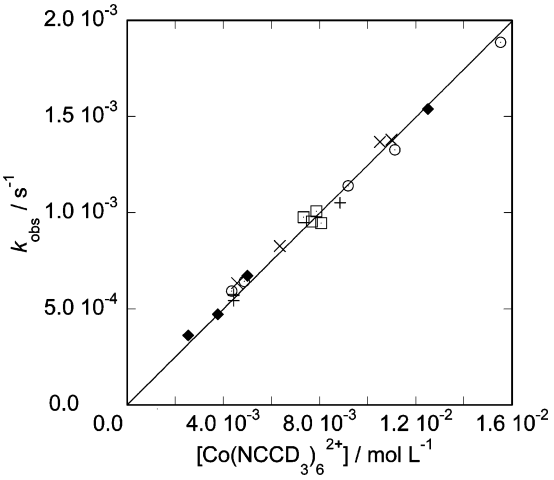

Figure 3. Catalyst concentration dependence of the observed rate constants in acetonitrile-d_3 at $T = 298.2$ K. (○) $Co(NCCD_3)_6^{2+}$ only, (□) $Co(NCCD_3)_6^{2+}$ and HOTf ≤ 0.10 mol L^{-1}, (+) $Co(NCCD_3)_6^{2+}$ and $Zn(NCCD_3)_6^{2+} \leq 4.8 \times 10^{-3}$ mol L^{-1}, (◆) $Co(NCCD_3)_6^{2+}$ and $FeCp_2 \leq 3.0 \times 10^{-3}$ mol L^{-1}, (×) $Co(NCCD_3)_6^{2+}$ and $Bu_4NPF_6 \leq 3 \times 10^{-3}$ mol L^{-1}.

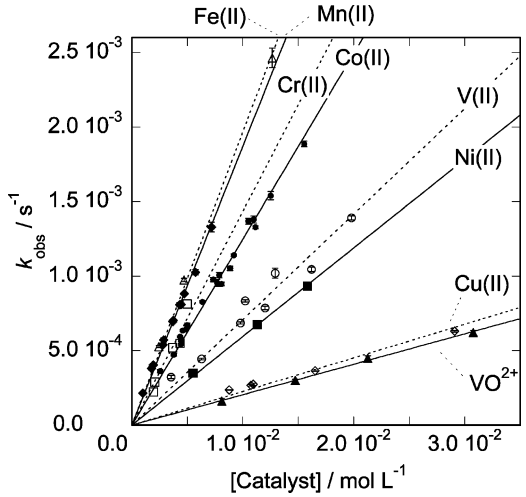

Figure 4. Plot of the observed nuclear spin interconversion rate constants against the catalyst concentrations at 298.2 K.

the observed rate constant also indicated the absence of medium effects from the variation of ionic strength.

$$\frac{\mathrm{d}[\textit{ortho}\text{-}\mathrm{H_2}]}{\mathrm{d}t} = k_{\mathrm{obs}}[\mathrm{Catalyst}] \qquad (2)$$

The dependences of k_{obs} on catalyst concentration are shown in Figure 4 for various divalent 3*d* transition metals. The slope of the lines in Figure 4 for each metal ion represents the second-order rate constant that is the sum of the forward and reverse rate constants applicable to eq 1. Following the convention in this area, the constant k^0 is tabulated in this study.

$$k^0 = k_{\mathrm{po}} + k_{\mathrm{op}} = 4.00k_{\mathrm{op}} = 1.33k_{\mathrm{po}} \qquad (3)$$

According to Wigner's theory[24] for the effect of paramagnets, the rate constant is controlled by the collision efficiency, $Z_{p\rightarrow o}$, as expressed in eq 4.

$$Z_{\mathrm{p}\rightarrow\mathrm{o}} = \frac{8\mu_{\mathrm{a}}{}^2\mu_{\mathrm{b}}{}^2 I\pi^2}{9h^2r^6k_{\mathrm{B}}T} \qquad (4)$$

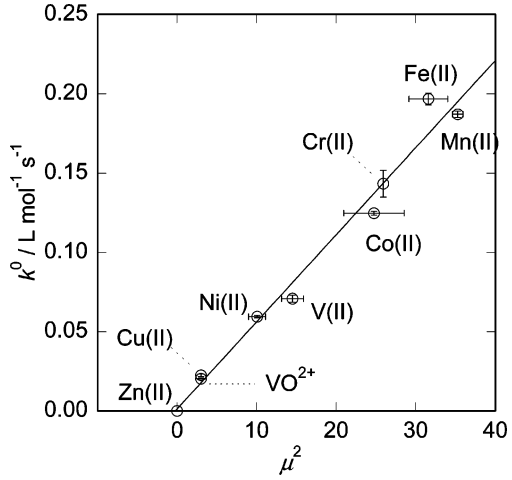

Figure 5. Plot of the rate constants against the square of the magnetic moment at 298.2 K in acetonitrile-d_3.

Table 1. Second-Order Rate Constants of *p*-/*o*-H_2 Spin Conversion and the Corresponding Magnetic Moments of the Dipositive 3*d* Metal Ions

catalyst	3*d* electron (*N*)[a]	magnetic moment/β	$k^0/10^{-2}$ L mol^{-1} s^{-1}
Mn(II)	5 (5)	5.94 ± 0.06[37,43]	18.7 ± 0.2
Fe(II)	6 (4)	5.62 ± 0.22[37,43,44]	19.7 ± 0.4
Cr(II)	4 (4)	5.09[37]	14.3 ± 0.8
Co(II)	7 (3)	4.97 ± 0.38[37,43,45,46]	12.5 ± 0.1
V(II)	3 (3)	3.81 ± 0.18[37,47−49]	7.1 ± 0.2
Ni(II)	8 (2)	3.17 ± 0.17[37,50,51]	5.94 ± 0.08
Cu(II)	9 (1)	1.73[b]	2.26 ± 0.08
VO^{2+}	1 (1)	1.73[b]	2.04 ± 0.02
Zn(II)	10 (0)	0[b]	$\leq 10^{-3}$

[a] Number of 3*d* electrons and, parenthetically, of unpaired electrons of given oxidation states. [b] Spin-only magnetic moments.

In eq 4, μ_a and μ_b are the magnetic moments of the paramagnetic species and of the proton; I is the moment of inertia of the hydrogen molecule; r is the collision distance; and S is a temperature-dependent distribution function. Wigner's equation suggests that the rate constants should be proportional to the squares of the magnetic moments of the catalysts and to the reciprocal of the sixth power of their collision distances.

Figure 5 presents a plot of k^0 against the square of the magnetic moment of each ion. The reported magnetic moments of $M(NCMe)_6^{2+}$ were used unless otherwise noted. It is important to use experimentally observed magnetic moments instead of spin-only values because the magnetic moments of the acetonitrile complexes of Fe, Co, and Ni often surpass the spin-only magnetic moments.[37] The second-order rate constants and magnetic moments are summarized in Table 1.

The linear correlation between k^0 and μ^2 in Figure 5 validates the Wigner equation and also suggests the collision distance between the H_2 molecule and these solvated complexes remains effectively constant. The latter point is an unexpected result because the metal to coordinating atom distances of $M(NCMe)_6^{2+}$ vary up to 15 pm, 222 pm for Mn(II)[38] and 207 pm for Ni(II),[39−42] which could cause substantial scatter in Figure 5. The Wigner theory predicts the rate constant is proportional to

(37) Buschmann, W. E.; Miller, J. S. *Chem.—Eur. J.* **1998**, *4*, 1731−1737.
(38) Weller, F.; Mai, H.-J.; Dehnicke, K. *Z. Naturforsch., B* **1996**, *51*, 298−300.
(39) Pietikainen, J.; Maaninen, A.; Laitinen, R. S.; Oilukaniemi, R.; Valkonen, J. *Polyhedron* **2002**, *21*, 1089−1095.
(40) Veith, M.; Godicke, G.; Huch, V. *Z. Anorg. Allg. Chem.* **1989**, *579*, 99−110.

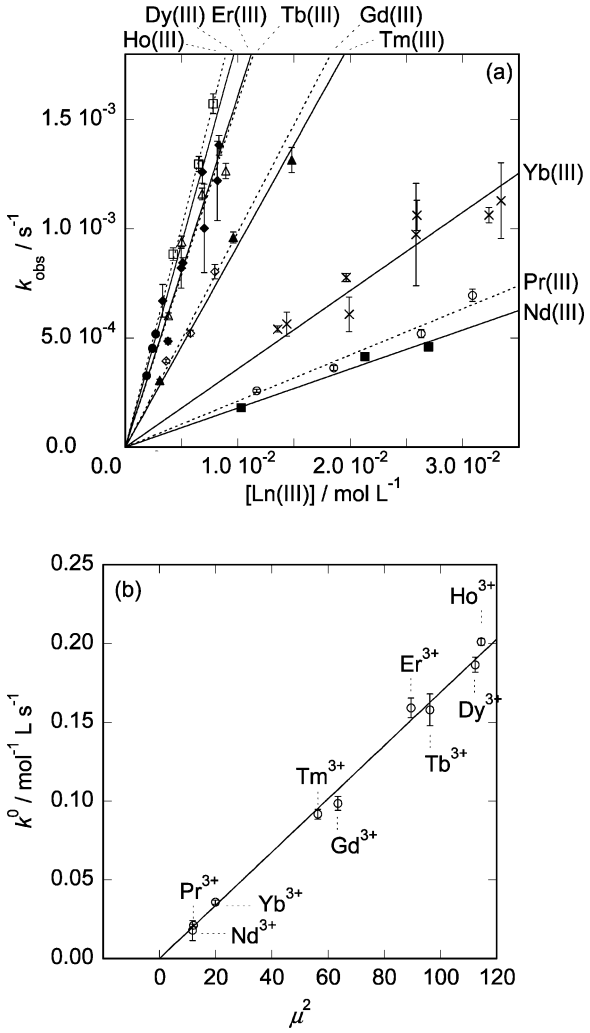

Figure 6. (a) Plots of the observed rate constants against concentrations of the catalysts and (b) second-order rate constants against the square of the magnetic moments; $T = 298.2$ K, in acetonitrile-d_3.

r^{-6}, therefore the difference of the rate constants between Mn(II) and Ni(II) should amount to a factor of $(k^0_{Mn(II)}/\mu^2)/(k^0_{Ni(II)}/\mu^2) = (r_{Mn(II)}/r_{Ni(II)})^{-6}$, or 1.52. Such an insensitivity of rate constants to the size of catalysts was also inferred by Wilmarth,[22] who used various Cr(III) complexes and concluded that their sizes do not affect the rate constants.

Spin Conversion Reactions with Lanthanide Complexes. To explore the effects of catalyst size on the rate constants, a series of lanthanide complexes was used as catalysts. Lanthanides have larger effective radii than 3*d* transition metals[52]

Table 2. Second-Order Rate Constants of *p*-/*o*-H_2 Spin Conversion and the Corresponding Magnetic Moments of the Trivalent Lanthanide Ion Catalysts

catalyst	4*f* electron (*N*)[a]	magnetic moment/β[b]	$k^0/10^{-2}$ L mol^{-1} s^{-1}
Gd(III)	7 (7)	7.97	9.85 ± 0.44
Tb(III)	8 (6)	9.81	15.8 ± 1.0
Dy(III)	9 (5)	10.6	18.6 ± 0.5
Ho(III)	10 (4)	10.7	20.1 ± 0.2
Er(III)	11 (3)	9.46	16.1 ± 0.6
Nd(III)	3 (3)	3.44	1.79 ± 0.08
Tm(III)	12 (2)	7.51	9.24 ± 0.37
Pr(III)	2 (2)	3.48	2.11 ± 0.08
Yb(III)	13 (1)	4.47	3.58 ± 0.13

[a] Number of 4*f* electrons and, parenthetically, of unpaired electrons for trivalent lanthanide complexes. [b] Magnetic moments of $Ln(NO_3)_3(phen)_2$ were used.[53]

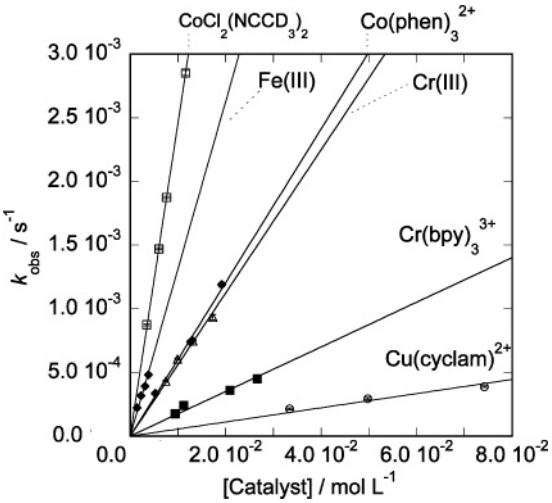

Figure 7. Plots of the observed rate constants against concentrations of the catalysts at $T = 298.2$ K, in acetonitrile-d_3.

that monotonically decrease with the number of *f*-electrons. Furthermore, the magnetic moments of Ln^{3+} vary over a wide range, up to 10.7 for Ho^{3+}.[53]

Besides unstable Pm, nine lanthanides were selected on the basis of the agreement between the calculated (Russell−Saunders) and observed magnetic moments.[54] Thus the rate constants for Ce, Pm, Sm, and Eu were not evaluated. The catalyst concentration dependences of observed rate constants are shown in Figure 6a. The correlation of the second-order rate constants k^0 and the squares of the magnetic moments μ is shown in Figure 6b. The resulting second-order rate constants are listed in Table 2. Once again the observed rate constants are proportional to the catalyst concentration and the second-order rate constant is proportional to the square of the magnetic moments. Despite the fact that Shannon's effective radius changes from 113 pm for Pr^{3+} to 100.8 pm for Yb^{3+}, no significant deviations were found in Figure 6b.

One notes from Figure 6b that the slope of k^0 vs μ^2 is obviously smaller for the lanthanide complexes than that for the divalent 3*d* transition metal complexes (Figure 5). When the magnetic moments are the same, 3*d* transition metals complexes can catalyze the *p*-/*o*-H_2 conversion more efficiently

(41) Leban, I.; Gantar, D.; Frlec, B.; Russell, D. R.; Holloway, J. H. *Acta Crystallogr.* **1987**, *C43*, 1888−1890.
(42) Sotofte, I.; Hazell, R. G.; Rasmussen, S. E. *Acta Crystallogr.* **1976**, *B32*, 1692−1696.
(43) Hathaway, B. J.; Holah, D. G.; Underhill, A. E. *J. Chem. Soc.* **1962**, 2444−2448.
(44) Hathaway, B. J.; Holah, D. G. *J. Chem. Soc.* **1964**, 2408−2416.
(45) Curzon, E. H.; Herron, N.; Moore, P. *J. Chem. Soc., Dalton Trans.* **1980**, 574−578.
(46) Leigh, G. J.; Sanders, J. R.; Hitchcock, P. B.; Fernandes, J. S.; Togrou, M. *Inorg. Chim. Acta* **2002**, *330*, 197−212.
(47) Anderson, S. J.; Wells, F. J.; Wilkinson, G.; Hussain, B.; Hursthouse, M. B. *Polyhedron* **1988**, *7*, 2615−2626.
(48) Kruck, T.; Kramolowski, R.; Hieber, W.; Winter, E.; Schubert, E. *Chem. Ber.* **1962**, *95*, 3070−3076.
(49) Janas, Z.; Jerzykiewicz, L. B.; Przybylak, S.; Richards, R. L.; Sobota, P. *Organometallics* **2000**, *19*, 4252−4257.
(50) Matwiyoff, N. A.; Hooker, S. V. *Inorg. Chem.* **1967**, *6*, 1127−1133.
(51) Hathaway, B. J.; Holah, D. G. *J. Chem. Soc.* **1964**, 2400−2408.
(52) Shannon, R. D. *Acta Crystallogr.* **1976**, *A32*, 751−767.
(53) Hart, F. A.; Laming, F. P. *J. Inorg. Nucl. Chem.* **1965**, *27*, 1605−1610.
(54) Aspinall, H. C. *Chemistry of the f-Block Elements*; Gordon and Breach: Amsterdam, 2001.

Table 3. Second-Order Rate Constants of *p*-/*o*-H_2 Spin Conversion and the Corresponding Magnetic Moments

catalyst	3*d* electron (*N*)[a]	magnetic moment/β	$k^0/10^{-2}$ L mol^{-1} s^{-1}
Fe(III)	5 (5)	5.49 [b]	13.1 ± 0.4
$[CoCl_2(NCCD_3)_2]$	7 (3)	4.59 [b]	24.6 ± 0.1
$[Co(phen)_3]^{2+}$	7 (3)	4.49 ± 0.15[55]	6.0 ± 0.1
$[Cr(NCCD_3)_6]^{3+}$	3 (3)	3.61 ± 0.01 [b]	5.6 ± 0.2
$[Cr(bpy)_3]^{3+}$	3 (3)	3.56[56]	1.75 ± 0.08
$[Cu(cyclam)]^{2+}$	9 (1)	1.60[57]	0.56 ± 0.03

[a] Number of 3*d* electrons and, parenthetically, of unpaired electrons of each complex. [b] Magnetic moments of $[Fe(OH_2)_6]^{3+}$,[58] $[CoCl_4]^{2-}$,[59] and $[Cr(OH_2)_6]^{3+}$ [60,61] were used, respectively.

compared to lanthanides. This result contradicted our prediction since the lanthanide complexes exist as $Ln(OD_2)_n^{3+}$ ($n = 8-9$) in 10% D_2O of CD_3CN solution and, according to Wigner's theory, smaller $Ln(OD_2)_n^{3+}$ should thus be a better catalyst rather than $M(NCCD_3)_6^{2+}$. In the following parts we further examine the effects from the nature of ligands, coordinating atom, and coordination number.

Nuclear Spin Interconversion Reactions with Other 3*d* Transition Metal Complexes. To extend the investigation, paramagnetic species with various ligands were used as catalysts. The catalyst concentration dependences of observed rate constants are shown in Figure 7, and the second-order rate constants are listed in Table 3.

For other 3*d* metal complexes with various ligands, the rate constant is moderately sensitive to the size of catalysts. By replacing coordinated acetonitrile-d_3 with bulkier ligands, the conversion rate constants of Co(II), Cr(III), and Cu(II) decreased. For example, the second-order rate constants for Cr(III) complexes decreased by a factor of 3.2 upon replacing coordinated acetonitrile-d_3 with 2,2′-bipyridine. The effect of the size of catalysts was smaller than that expected from Wigner's theory. When van der Waals radii of $Co(NCCD_3)_6^{2+}$, 500 pm, and $Co(phen)_3^{2+}$, 700 pm,[62,63] were applied to the Wigner's equation, the calculated ratio of the second-order rate constants between those two Co(II) complexes was 9.2 (eq 5); whereas, the experimentally estimated ratio was merely 2.1.

$$\frac{k^0_{\mathrm{Co(NCCD_3)}}}{k^0_{\mathrm{Co(phen)}}} = \left(\frac{\mu_{\mathrm{Co(NCCD_3)}}}{\mu_{\mathrm{Co(phen)}}}\right)^2 \left(\frac{r_{\mathrm{Co(phen)}}}{r_{\mathrm{Co(NCCD_3)}}}\right)^6 \qquad (5)$$

Measurements in D_2O and Dimethylformanide-d_7. Preliminary measurements in D_2O and dimethylformamide-d_7 were carried out (data in the Supporting Information). As mentioned in the Experimental Section, the accuracy of kinetic measurements in D_2O suffered from the low solubility of H_2 and the interference from the solvent's peak. The second-order rate constants of the conversion reaction in D_2O and DMF-d_7 were compared with those in acetonitrile-d_3 in Figure 8.

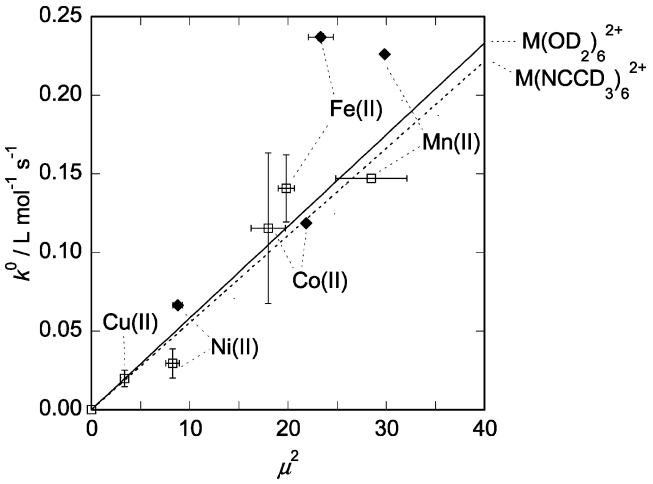

Figure 8. Plots of second-order rate constants against the square of the magnetic moments in D_2O (□), in dimethylformamide-d_7 (◆), and the solid line is the k^0 vs μ^2 correlation in aceotonitrile-d_3 (see Figure 5).

Table 4. Collision Distance, *r*, for Various Metal Catalysts, Calculated from k^0

catalyst	*N*[a]	*r*/pm	catalyst	*N*[a]	*r*/pm	catalyst	*N*[a]	*r*/pm
Mn(II)	5	351	Gd(III)	7	431	$Fe(solv)^{3+}$	5	363
Cr(II)	4	348	Tb(III)	6	427	$Cr(NCCD_3)_6^{3+}$	3	363
Fe(II)	4	342	Dy(III)	5	426	$Cr(bpy)_3^{3+}$	3	439
V(II)	3	359	Ho(III)	4	422	$CoCl_2(NCCD_3)_2$	3	308
Co(II)	3	354	Er(III)	3	420	$Co(phen)_3^{2+}$	3	386
Ni(II)	2	345	Nd(III)	3	433	$Cu(cyclam)^{2+}$	1	408
Cu(II)	1	331	Pr(III)	2	422			
$V^{IV}O^{2+}$	1	337	Tm(III)	2	427			
			Yb(III)	1	420			

[a] Number of unpaired electrons.

Even though a large error exists for the measurements in D_2O, the slope of k^0 vs μ^2 in D_2O agreed with that in acetonitrile-d_3. This result indicates the reactivity of $M(OD_2)_6^{2+}$ and $M(NCCD_3)_6^{2+}$ for the *p*-/*o*-H_2 conversion or the collision distances between those complexes and an H_2 molecule are the same. In DMF-d_7, the correlation of k^0 vs μ^2 for $Ni(DMF\text{-}d_7)_6^{2+}$ and $Co(DMF\text{-}d_7)_6^{2+}$ agreed reasonably with that in the other solvents. The large deviations found for $Fe(DMF\text{-}d_7)_6^{2+}$ and $Mn(DMF\text{-}d_7)_6^{2+}$ may be the result of the magnetic moments, which might be different than assumed.[64−68]

All solvated complexes with 3*d* transition metal centers have the same k^0 vs μ^2 correlation; therefore the second-order rate constants depend only on the magnetic moments and not on the size of ligands, or the coordinating atoms.

Calculation of Collision Distances. Since the conventional radii such as van der Waals or Shannon's Effective values do not fit the collision distance of the Wigner theory, we estimated the collision distance from the second-order rate constants and magnetic moments. Wilmarth had also calculated the collision distance by the same manner by reducing the Wigner theory to a simple form, $r = 146(\mu^2/k^0)^{1/6}$: r in pm, k^0 in L mol^{-1} s^{-1}.[22] His conclusion was, however, that no clear correlation exists

(55) Geraghty, M.; McCann, M.; Devereux, M.; McKee, V. *Inorg. Chim. Acta* **1999**, *293*, 160−166.
(56) Perthel, R. *Z. Phys. Chem.* **1959**, *211*, 74−78.
(57) Shakir, M.; Varkey, S. P.; Nasman, O. S. M. *Indian J. Chem.* **1996**, *A35*, 671−676.
(58) Fedotov, M. A.; Taraban, E. A.; Zaikovskii, V. I.; Ignashin, S. V.; Buyanov, R. A. *Russ. J. Inorg. Chem.* **1998**, *43*, 388−393.
(59) Cotton, F. A.; Wilkinson, G.; Murillo, C. A.; Bochmann, M. *Advanced Inorganic Chemistry*, 6th ed.; Wiley-Interscience: New York, 1999.
(60) Thompson, M.; Connick, R. E. *Inorg. Chem.* **1981**, *20*, 2279−2285.
(61) Rajasekar, N.; Subramaniam, R.; Gould, E. S. *Inorg. Chem.* **1982**, *21*, 4110−4111.
(62) Grace, M. R.; Swaddle, T. W. *Inorg. Chem.* **1993**, *32*, 5597−5602.
(63) Sachinidis, J. I.; Shalders, R. D.; Tregloan, P. A. *Inorg. Chem.* **1996**, *35*, 2497−2503.
(64) Prabhakaran, C. B.; Patel, C. C. *J. Inorg. Nucl. Chem.* **1968**, *30*, 867−869.
(65) Khutornoi, V. A.; Naumov, N. G.; Mironov, Y. V.; Oeckler, O.; Simon, A.; Fedorov, V. E. *Russ. J. Coord. Chem.* **2002**, *28*, 183−190.
(66) Gritzner, G.; Linert, W.; Gutmann, V. *J. Inorg. Nucl. Chem.* **1981**, *43*, 1193−1200.
(67) Matwiyoff, N. A. *Inorg. Chem.* **1966**, *5*, 788−795.
(68) Nortia, T. *Suom. Kemistil. B* **1962**, *35*, 169−170.

Scheme 1. Distances between a Metal Center and Atoms in Coordinated Ligands: $Co(NCCMe)_6^{2+}$ [40,69,70] and $Pr(OH_2)_9^{3+}$ [74–76]

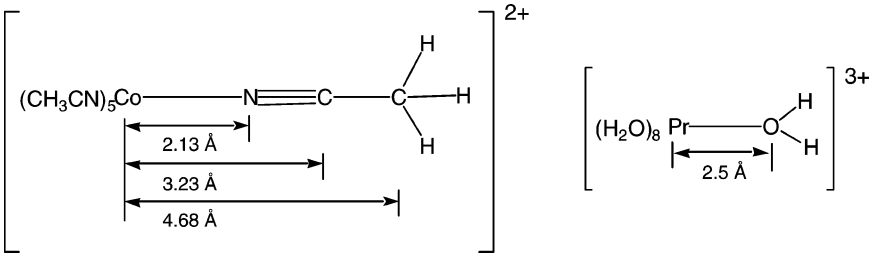

between k^0 and the size of catalyst. We present the calculated collision radii in Table 4.

As expected from the good linear correlations between k^0 and μ^2 for the solvated complexes of both 3*d* transition metals and lanthanides, the calculated collision distances were constant for each series.

For the solvated 3*d* transition metal complexes the estimated collision radius is ~350 pm. Relatively small distances for Cu(II) and VO^{2+} at *N* (number of unpaired electron) = 1 compared to other solvated 3*d* transition series may be due to the use of spin-only magnetic moments. Considering the error in the magnetic moments of $[Fe(solv)]^{3+}$ and $[Cr(NCCD_3)_6]^{3+}$, trivalent solvated 3*d* transition metal complexes share the same collision distance, too. On the other hand, the lanthanide complexes resulted in a larger collision distance ~425 pm. Within the lanthanide series, the calculated collision distance might reflect Shannon's Effective Radius: heavy lanthanides resulted in a somewhat smaller collision radius compared to light lanthanides.

The distance parameters from the crystal structures of $Co(NCCMe)_6^{2+}$ and $Pr(OH_2)_9^{3+}$ are depicted in Scheme 1. The calculated collision distance of $Co(NCCMe)_6^{2+}$, 350 pm, appeared to lie just outside of the C–N triple bond,[40,69,70] which indicated that a H_2 molecule penetrates the first coordination shell to interact with the unpaired 3*d* electron of the Co(II) center. Such close contact has been suggested for the *p*-/*o*-H_2 conversion reactions in heterogeneous media (H_2 gas/solid surface), because the rate constants on solid surfaces usually surpass the prediction from Wigner theory.[11,71] Partial molar volume[63,72] or diffusion coefficients[73] of metal complexes often indicate close interactions between a metal complex and solvent molecule. However, this close interaction model did not fit for the lanthanide complexes; the calculated collision radius was ca. 425 pm, which is apparently outside the first coordination shell.

The calculated collision distances for $[Ln(OD_2)_n]^{3+}$ and $[M(NCCD_3)_6]^{2+}$ contradict the van der Waals radii, which cannot be attributed to steric effects, the difference of coordinating atoms, or the charge of the metal center. The larger coordination number of lanthanides has little shielding effect on the collision between a lanthanide metal center and a H_2 molecule because the large effective radius of lanthanides provides enough exposure of the metal center to the H_2 molecule. The difference of coordinating atoms may be minimal because most of $[M(OD_2)_6]^{2+}$, $[M(DMF\text{-}d_7)_6]^{2+}$ result in the same k^0 vs μ^2 profile of $[M(NCCD_3)_6]^{2+}$ (Figure 8).

Scheme 2. Key Contributions for the Spin Conversion Rate Constant

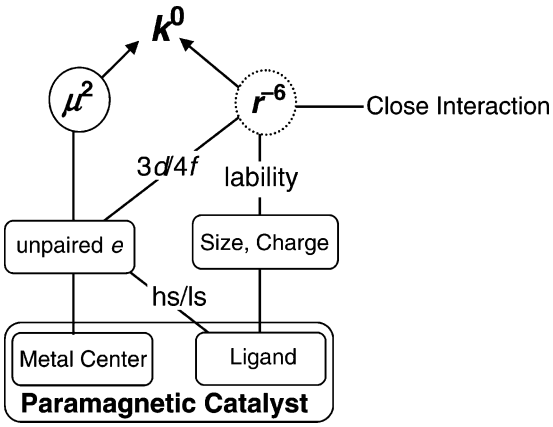

The difference of the collision distance between 3*d* metals and lanthanides may arise from electronic orbitals in which the unpaired electrons reside. For all 3*d* transition metal complexes, whether coordinated by solvent molecules or other ligands, the calculated collision distance fell short of van der Waals radii, whereas the collision distance of the lanthanide complexes indicated the second coordination shell. Relatively low catalytic efficiency, k^0/μ^2, and hence large collision distance of lanthanide oxides were also reported for the *p*-/*o*-H_2 conversion reactions on solid surface.[11,77] The collision distance of a metal complex and a hydrogen molecule may reflect the spatial fluctuation of an unpaired electron of the metal center.

For the other 3*d* transition metal complexes with other ligands, the collision distance varied from the smallest 308 pm of $[CoCl_2(NCCD_3)_2]$ to the largest 439 pm of $[Cr(bpy)_3]^{3+}$. Unlike the solvated complexes, the collision distances reflect the size of coordinating ligands. For Co(II), Cr(III), Cu(II), all result in larger collision distances by the coordination of bulky ligands. This trend supports the Wigner theory; however, $[Cr(bpy)_3]^{3+}$ has a much larger collision distance than $[Co(phen)_3]^{2+}$ despite their similar van der Waals radii.[63,78] We assume the substitution lability of a metal complex also affects the collision distance: substitution lability may facilitate access of a H_2 molecule to a metal center.

The charge of a ligand seems to have a stronger impact on the *p*-/*o*-H_2 conversion reactivity compared to the charge of

(69) Malkov, A. E.; Fomina, I. G.; Sidorov, A. A.; Aleksandrov, G. G.; Egorov, I. M.; Latosh, N. I.; Chupakhin, O. N.; Rusinov, G. L.; Rakitin, Y. V.; Novotortesev, V. M.; Ikorskii, V. N.; Eremenko, I. L.; Moiseev, I. I. *J. Mol. Struct.* **2003**, *656*, 207–224.
(70) Cotton, F. A.; Daniels, L. M.; Jordan, G. T., IV; Murillo, C. A. *Polyhedron* **1988**, *17*, 589–597.
(71) Farkas, L.; Sandler, Y. L. *J. Chem. Phys.* **1940**, *8*, 248–251.
(72) Matsumoto, M.; Tarumi, T.; Takahashi, I.; Funahashi, S.; Noda, T.; Takagi, H. D. *Z. Naturforsch.* **1997**, *52B*, 1087–1093.
(73) Pyati, R.; Murray, R. W. *J. Am. Chem. Soc.* **1996**, *118*, 1743–1749.
(74) Albertsson, J.; Elding, I. *Acta Crystallogr.* **1977**, *B33*, 1460–1469.
(75) Gerkin, R. E.; Reppart, W. J. *Acta Crystallogr.* **1984**, *C40*, 781–786.
(76) Chatterjee, A.; Maslen, E. N.; J., W. K. *Acta Crystallogr.* **1988**, *B44*, 381–386.
(77) Buyanov, R. A. *Kinet. Catal.* **1960**, *1*, 578–581.
(78) Hupp, J. T.; Weaver, M. J. *J. Phys. Chem.* **1985**, *89*, 2795–2804.

metal center. $[Fe(solv)]^{3+}$ and $[Cr(NCCD_3)_6]^{3+}$ have showed the same catalytic efficiency, k^0/μ^2, as the divalent 3*d* transition metal complexes do. On the other hand, tetrahedral $[CoCl_2(NCCD_3)_2]$ showed a much higher catalytic ability than any other solvated complexes. Since the effects from the catalyst's size are moderate for solvated Co(II) complexes, the negatively charged Cl^- ligand may enhance the catalytic ability. In Wilmarth's report, although he did not comment on the point, there is a trend that the Cr(III) complexes increase the *p*-/*o*-H_2 conversion reactivity by the coordination of negatively charged ligands; e.g., $k^0([Cr(SCN)_6]^{3-})$ is 6 times larger than $k^0([Cr(NH_3)_6]^{3+})$.[22]

Although more detail and sustainable explanation with theoretical standpoints must be needed, we suggest the factors contribute to the rate constant of spin conversion (Scheme 2).

The *p*-/*o*-H_2 nuclear spin isomerization reaction rate constant, k^0, is apparently a function of magnetic moments and collision distances. The good correlations shown between k^0 and μ^2 for solvated complexes validate the Wigner theory, and all reactions are considered to proceed through a collision mechanism. The reciprocal of the sixth power of collision distance, on the other hand, is difficult to prove at this point because the conventional molecular radius cannot be applied here. The magnetic moment is affected mostly from the number of unpaired electrons, and the coordinating ligand changes the spin configuration (high/low spin) of a metal center.

The factors that contribute to the collision distance are more complicated. At first, the collision distance is strongly influenced by the orbital in which the unpaired electrons reside. The unpaired electrons in 4*f* orbitals show less catalytic efficiency or interact with a H_2 molecule at longer collision distances compared to the electrons in 3*d* orbitals. The size and charge of coordinating ligands affect the collision distance as well: a small and negatively charged ligand can increase the catalytic efficiency. Such ligand effects may, however, be weakened when the catalyst is substitution labile (e.g., $[Co(phen)_3]^{2+}$). Even if the complex is substitution inert (e.g., $[Cr(bpy)_3]^{3+}$), the effects from the ligand size may be reduced, because a H_2 molecule can penetrate the inside of the first coordination shell and interact with the unpaired electron of the metal center. As a result the *p*-/*o*-H_2 conversion rate constant k^0 does not exhibit an apparent dependence on the size of paramagnetic catalysts.

Conclusions

The rate constants for para-/orthohydrogen nuclear spin isomerization were determined for wide ranges of metal complexes in deuterated solvents by using ^1H NMR spectroscopy. Excellent correlations between k^0 and μ^2 were shown for solvated 3*d* transition metals and lanthanide complexes, which prove the reaction proceeds through a collision mechanism and validates the Wigner theory. It is also noteworthy that the collision radii of a series of 3*d* transition metal complexes, or those of lanthanide complexes, are practically constant.

Collision distances were calculated based on Wilmarth's adaptation of the Wigner theory, which indicates that close interaction between the paramagnetic metal centers and molecular hydrogen is required. On the other hand, the calculated collision distances indicate that the interaction occurs outside the first coordination sphere of $Ln(OD_2)_n^{3+}$. At this point, the molecular interpretation of such collision distances remains open for discussion. To make a comprehensive explanation, a new criterion for collision distance may be needed.

Acknowledgment. This work was supported by the National Science Foundation, Grant CHE-020409. Some of the research was carried out in facilities of the Ames Laboratory which is operated for the U.S. Department of Energy by Iowa State University under Contract W-7405-Eng-82.

Supporting Information Available: Observed rate constants as a functions of the catalyst concentration (Table S1−S5) and the magnetic moments of $M(solv)_6^{2+}$; solv = H_2O or dimethylformamide (Table S6). This material is available free of charge via the Internet at http://pubs.acs.org.

JA0524292